



Particle Swarm Optimization Based Dual -Mode Fractional Order Control for Automatic Generation Control of Two Area Interconnected Hybrid System

Srivishnupriya Arumugasami Pavadaisami^{1*} Mohamed Thameem Ansari Musthafa¹
 Vinoth Kumar Natanmai Jeganathan²

¹*Department of Electrical Engineering, Annamalai University, Annamalai Nagar 608002, Tamil Nadu, India*

²*Department of Electrical and Electronics Engineering, Government Polytechnic College,
 Konam, Nagercoil 629004, Tamil Nadu, India*

* Corresponding author's Email: vishnuap28@gmail.com

Abstract: This research work presents a particle swarm optimization (PSO) based dual mode fractional order controller (PDMFOPI) to overcome the load frequency (LF) problem in two area interconnected hybrid systems (TAIHS). The proposed controller provides a high degree of freedom in tuning the controller because of the way it provides high control over the system. The fractional order controller, in combination with the dual mode scheme, increases the performance of the system. The gains of the controller are fine-tuned by a meta-heuristic particle swarm optimization algorithm in such a way as to minimize the error in the integral square error (ISE) criterion. To realize the controller advantages, a comparison is made between the proposed controller and other controllers of the conventional proportional-integral controller (PI), the PSO tuned dual mode proportional-integral controller (PDMPI), and the PSO tuned fractional order controller (PFOPI), all tested for the same system for 1% step load perturbation (SLP). Also, sensitivity and performance analyses are carried out. From the findings, it is clear that the suggested controller is efficient and clears frequency error in a short time.

Keywords: Two area interconnected hybrid power system (TAIHS), Load frequency control (LFC), Dual-mode scheme, Fractional order controller, Particle swarm optimization (PSO).

1. Introduction

Nowadays, our traditional system of electricity is being upgraded by incorporating generation sources of different types. Contrarily, demand will never be constant. It may increase or decrease at any time. As it is dynamic, it is essential to keep the generation and demand of power in synch; otherwise, frequency deviation may occur which leads to serious problems like blackouts. Therefore, the power system must be operated at a specified frequency all the time. For the purpose of keeping a balance between demand and generated power, load frequency control (LFC) is implemented. Maintaining regulation using old techniques is not feasible in the case of a large interconnected power system. As a result, automatic generation controllers are installed in each power plant. Here, optimized parameters are given as inputs

to the controllers to improve the system performance. Thus, for a small load change, the controller will operate and maintain the system with constant frequency. A power system is robust when the frequency and voltage remain constant regardless of load fluctuations. LFC stands for active power and frequency control. LFC is a major challenge for a multi-area integrated power system. [1]. Different types of microgrid systems have been developed and their dynamic characteristics studied by various authors. An isolated microgrid comprising a PV, wind, biogas, and biodiesel generator is addressed in [2]. The authors discussed the impacts of inexhaustible energy sources of photovoltaic (PV), hydroelectric plant and wind turbine generator after integration with exhaustible energy resources [3]. The frequency control of a microgrid comprising of the different generating system is studied, and a

mathematical model for different generation sources is also represented in [4]. Whereas in [5], an isolated hybrid power system consisting of wind turbine, aqua electrolyzer, diesel, electrical vehicle, PV, and flywheel energy storage systems is simulated. Aside from the many types of hybrid power systems outlined above, adding a high-voltage direct current (HVDC) tie line to the system, as well as an AC tie line, is a smart idea from both an economic and technical standpoint. In [6], a parallel HVDC tie-line is also modeled to mitigate the mismatched frequency because of the incorporation of different generating sources. A multi-terminal HVDC system for wind farm-connected multi-source power systems is modelled [7]. Moreover, different types of optimization techniques are implemented for the LFC problem. Different computational methods are being used in research to improve the accuracy and efficiency of LF management algorithms. In [8], the Harris Hawk's optimizer for solving the frequency constrain issues are discussed. Even after the development of many algorithms from the genetic algorithm [9] to recent algorithms like the Archimedes optimization [10], PSO is providing better results with simple procedures. To optimize the settings of the PID (proportional derivative integral) controller in the micro-grid structure, PSO based on an artificial neural network technique is utilized in [11]. Nowadays, various control approaches have been developed and are used for frequency control. For LFC functionality, new control approaches and intelligent methodologies have been presented, such as a linear quadratic regulator with an integral controller and online tuning using the balloon effect [12], the sliding mode controller [13], and coefficient diagram methods implemented for frequency control [14]. Although they are intelligent, due to some limitations and complex computation, classical methods are used for their simplicity. For instance, [15] proposes optimizing a PID controller's Ziegler-Nichols's tuning. In terms of research, it appears that advancements in design methodologies for integer order control, particularly PID control, have hit their limits. There are still some challenging issues to be resolved [16]. The integral and derivative actions' fractional-ordering results in the fractional order proportional integral derivative (FOPID) controller, which is an enhancement of the classical PID. As a result, the controller has two additional parameters than a traditional PID controller. As a result, two more standards must be met in order to increase the entire system's performance. Many engineering control applications have employed the controller to produce more robust and steady performance [17]. Various literature is available for the FO system in

frequency regulation. FO controllers manage frequency in a multi-area power system [18]. Also, FO controllers are used for AC microgrid frequency mitigation [19]. A fuzzy-logic-incorporated FO controller is applied in [20, 21]. In the above-discussed literature, it is understandable that various types of power system with renewable energy is modeled which is highly encouraged. But it is a fact that systems incorporating renewable energy become more complex systems due to their dynamic behavior. Thus, for a complex system, a complex method of control is not suitable. Like fuzzy systems, and neural networks, they require experts to design the controller and may be time-consuming. Also, older control techniques of Conventional PI control not resolve the issue between static and dynamic accuracy, the closed-loop system's gain can be adjusted significantly to improve transient response in the absence of integral control. Also, in the above-reported works of literature, various algorithms implemented in tuning controllers have some limitations of slow convergence, more settling time and stuck in local optima. The motivation of this work is to design a most effective simple controller by overcoming above discussed drawbacks. The problem can be handled by enhancing the dual-mode control paradigm [22]. This dual-mode control does not include any complex structure and it is easy to implement [23]. These controllers are robust and less sensitive to system variations [24]. For that purpose, a facile and efficient dual mode fractional order proportional-integral controller tuned by a simple and uncomplicated PSO algorithm (PDMFOPI) is proposed for tuning a complex two area hybrid power system incorporating different renewable energy sources. For the purpose of proving the efficacy of the proposed controller it is compared with different controllers of conventionally tuned PI controller and PSO tuned dual PI and FOPI controller. The organization of further work is, in Section 2 explains the contribution of the article. Section 3 is associated with the system investigated and its mathematical modeling. Section 4 explains the fractional order controller. Section 5 is associated with the dual-mode scheme and the problem formulation of the work. Section 6 deals with the PSO algorithm. Section 7 is associated with the design of gain scheduling controllers. And finally, Section 8 is associated with observation and results obtained in the form of waveform and numerical data and Results, and finally Section 9 is the conclusion.

2. Contribution of the article

All In this work a most advantageous design of PSO-based dual-mode PI controller (PDMFOPI) is proposed for the TAIHS. Along with its desirable characteristics of design simplicity and ease of implementation, the PSO-based dual-mode system is implemented for fractional proportional integral (PI) controller for the TAIHS.

The following are the work's aims:

- TAIHS integrating different generation sources is considered to be controlled.
- A PDMFOPI is incorporated because of its good performance and greater freedom in tuning.
- A PSO algorithm to tune the controller parameter is implemented because it is simple to understand, easy to execute, and cost-effective.
- The system also contains an HVDC link in addition to an AC tie line for frequency regulation.
- Sensitivity analysis is performed by taking into account various operational circumstances and load disturbances.

3. System investigated

To provide a robust design methodology for the power system LFC, the PSO-based dual-mode fractional order proportional-integral (PDMFOPI) idea was applied. Fig. 1 depicts a one-line diagram of TAIHS with a hydro plant, reheat thermal plant and gas plants in one area and diesel plant, wind plant, and solar plant in the other. Also, a nonlinear Generation Rate Constraint (GRC) is added to the thermal power; thus, it acts as real power system. For small SLP the change in power of different generation units is given below from in Eqs. (1) to (6). And from Eqs. (7) to (13) refers to power flow equations of area 1, area2, AC and HVDC tie-line power of TAIHS [25] and the nominal data of the TAIHS is supplied in Appendix A.

Thermal plant:

In Eq. (1), K_{RE} is gain constant of reheat turbine whereas T_{TR} , T_{GR} , T_{RE} are the time constant of a turbine, governor, reheat turbine.

$$\Delta P_{th}(s) = \frac{(1+K_{RE}T_{RE}S)}{(1+T_{GR}S)(1+T_{RE}S)(1+T_{TR}S)} \quad (1)$$

Hydro plant:

In hydro turbine transfer function Eq. (2), T_{RS} is the reset time, T_W is the water flow starting time in penstock, T_{RH} is the hydro governor time constant.

$$\Delta P_{hy}(s) = \frac{(1+T_{RS}S)(1-T_W S)}{(1+T_{HS}S)(1+T_{RHS}S)(1+0.5T_W S)} \quad (2)$$

Gas plant:

In Eq. (3), A , B , C are the constants of valve positions. T_{CD} , T_{CR} and T_F are the time constants of compressor discharge, combustion reaction and fuel.

$$\Delta P_{ga}(s) = \frac{A(1+XS)(1-T_{CR}S)}{(C+BS)(1+YS)(1+TFs)(1+T_{CD}S)} \quad (3)$$

Diesel plant:

In Eq. (4), K_D is the gain constant and T_{D1} , T_{D2} , T_{D3} , T_{D4} are the time constants of the diesel plant.

$$\Delta P_{di}(s) = \frac{K_D(1+T_{D1}S)}{(1+T_{D4}S)(1+T_{D2}S)(1+T_{D3}S)} \quad (4)$$

Wind plant:

In wind plat transfer function Eq. (5), K_{W1} and K_{W2} are the gain constant and T_{W1} and T_{W2} are the time constants of wind turbine.

$$\Delta P_{wi}(s) = \frac{K_{W1}K_{W2}(1+T_{W1}S)}{(1+T_{W2}S)(1+2S+S)} \quad (5)$$

Solar PV plant:

In Eq. (6), K_{PV} is the gain constant and T_{PV} is the time constant of PV plant.

$$\Delta P_{PV}(s) = \frac{K_{PV}}{1+T_{PV}S} \quad (6)$$

For change in generation due to load change, the total power generated is given by

For area1

$$\Delta P_{GEN1} = \Delta P_{th} + \Delta P_{hy} + \Delta P_{ga} \quad (7)$$

For area2

$$\Delta P_{GEN2} = \Delta P_{di} + \Delta P_{wi} + \Delta P_{pv} \quad (8)$$

Since in parallel to AC tie line, the HVDC line also considered. Therefore, the total tie line power is given by

$$\Delta P_{tie12} = \Delta P_{tac} + \Delta P_{tdc} \quad (9)$$

$$\Delta P_{tac} = (T_{12})\Delta P_{tac} + \Delta P_{tdc} \quad (10)$$

$$\Delta P_{tdc} = \frac{K_{tdc}}{1+T_{dc}}(\Delta F1 - \Delta F2) \quad (11)$$

In AC tie-line, T_{12} is the synchronizing coefficient. The disparity between scheduled and actual power is mentioned as area control error (ACE). ACE provided by this parallel AC and DC tie line is

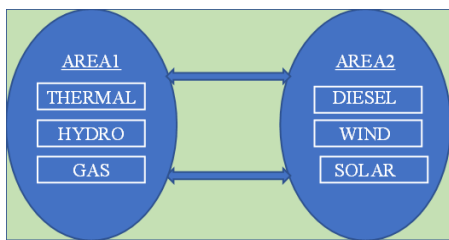


Figure. 1 One-line diagram of TAIHS

For area1

$$ACE_{A1} = B1 \Delta F1 (\Delta P_{tac} + \Delta P_{tdc}) \quad (12)$$

For area2

$$ACE_{A2} = B2 \Delta F2 (\Delta P_{tac} + \Delta P_{tdc}) \quad (13)$$

4. Fractional order controller

Podlubny first suggested the concept of fractional order controllers in 1997. It states that it has a better response compared with conventional PID controller. The FO controller is an effective control method for preventing unwanted instability and improving the dynamic behaviour of the power system model. New tuning methods are being developed and also the applications of FO controller are being investigated [26]. Fractional order differential equations are used to access systems in fractional order control. Fractional calculus is used by fractional order controllers to extract their lineage. The controller's transfer function is given by

$$u(t) = K_p e(t) + \int_0^t \frac{K_i}{s^\lambda} e(t) \quad (14)$$

In Eq. (14), $u(t)$ represents the produced control signal and $e(t)$ denotes the error signal. As a result, the controller includes a proportional component gain, an integral component gain, and a fractional operator λ . The FOPI controller is derived from the integer order PI controller. Similarly, a traditional PI controller is created by changing the value to 1. As a result, the controller includes a proportional component gain, an integral component gain, and a fractional operator λ . By adjusting the value between 0 and 1, the design specifications can be changed [27].

5. Dual mode scheme and problem formulation

This section explains the dual mode concept followed by problem formulation.

5.1 Dual mode scheme Implementation

A well-designed proportional or integral controller can achieve 0% steady state error, but the system's response becomes delayed as a result of the high overshoot and undershoot and makes up time. The notion of a dual-mode scheme can be used to resolve this contradiction. In this technique, a dual-mode switch is used to link one of two controllers to the feedback loop at a time. The structure of PDMFOPI controller is shown in Fig.3. The first controller is driven by a linear feedback law, whereas the second is driven by a state transition. Thus, the PDMPI controller switches between proportional and integral control according to the Eqs. (15) and (16) and for the PDMFOPI controller it works with respect to Eqs. (15) and (17). In Eq. (17) λ is a fractional operator which has a value between 0 and 1 for which it acts as FOPI controller. When the $\lambda = 1$, then it will act as a conventional proportional integral controller as in Eq. (16). The modes of the controller depend on the output signal level.

$$u(t) = K_p e(t) \text{ for } |e(t)| = ACE > \varepsilon \quad (15)$$

$$u(t) = \frac{K_i}{s} e(t) \text{ for } |e(t)| = ACE \leq \varepsilon \quad (16)$$

$$u(t) = \frac{K_i}{s^\lambda} e(t) \text{ for } |e(t)| = ACE \leq \varepsilon \quad (17)$$

Where ε is the specified switching limit, which must be greater than 0. That is, $\varepsilon > 0$. When the amplitude of the error $e(t)$ is more than the defined value, the proportional scheme is employed, and when the amplitude of the error $e(t)$ is less than or equal to, integral control is used.

5.2 Problem formulation

To minimize (J) is the primary goal of LFC problem. Here, Eq. (18) is the integral square error of frequency change and tie line power change with subject to constraints as in Eq. (19) which are the minimum and maximum bounds of the variables to be tuned.

$$J_{ISE} = \int_0^t \{(\Delta F_i)^2 (\Delta P_{tie12})^2\} dt \quad (18)$$

with subject to constraints,

$$\begin{cases} K_{pmin} \leq K_p \leq K_{pmax} \\ K_{imin} \leq K_i \leq K_{imax} \\ \lambda_{min} \leq \lambda_i \leq \lambda_{max} \\ \varepsilon_{min} \leq \varepsilon_i \leq \varepsilon_{max} \end{cases} \quad (19)$$

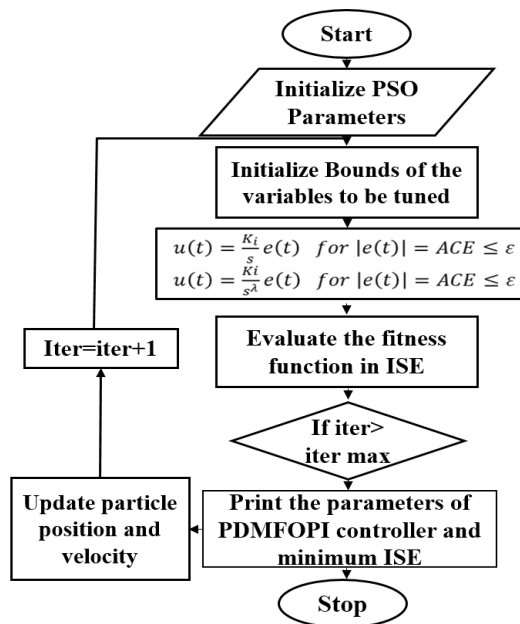


Figure. 2 Flow chart of PSO algorithm

The basic goal of the LFC problem is to keep the frequency and power deviations as low as possible. The integral square error (ISE) is a performance metric that can be used to find the best controller parameters [28]. A PSO is used to help with this. PSO is a very simple algorithm that appears to work well for optimizing a variety of functions. The technique for adjusting the controller's gains is explained in the following sections.

6. Particle swarm optimization algorithm

James Kennedy introduced PSO, which states a group of flying birds or fish searching for food. In this algorithm, the solution to be obtained is termed as a particle. According to the Eqs. (20) and (21) each particle will have two vectors that determine its position in the search space: a position vector and a velocity vector. In search space, each particle moves toward two points, namely P_{KBEST} and G_{KBEST} , where P_{KBEST} is the optimum solution obtained by each single particle, and G_{KBEST} , is the optimum solution obtained by all the particles. Each particle can be thought of as a massless point in z-dimensional space, indicated by z in a group of particles. Thus, particles move with velocity toward the optimum solutions. For j^{th} iteration, the updated velocity of the particle x is given by

$$v = Wv_{pi}^j + C_1R_{a1}(P_{KBESTi} - x^{j-1}_{iz}) + C_2R_{a2}(G_{KBESTi} - x^{j-1}_{iz}) \quad (20)$$

were,

$$x_{iz}^j = x_{iz}^{j-1} + v_i^j \quad (21)$$

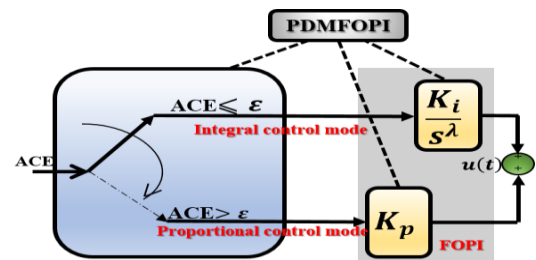


Figure. 3 Structure of PDMFOPI controller

Table 1. PSO parameters

Parameter	value
No of population	30
No of iteration	50
Learning factor	2
Inertia coefficient upper and lower limits	0.9 and 0.2

W is the inertia coefficient representing the search ability, C_1 and C_2 are learning factors whose values are greater than 1, R_{a1} and R_{a2} are random values between 0 and 1. Fig. 2 illustrates the flow chart of a PSO for the gain scheduling for an interconnected hybrid power system. According to this, after initialising PSO parameters and controller boundaries, we can achieve our main goal of decreasing the performance index J given in Eq. (18) by using optimum values of controller gains achieved by particle movement in the search space. The following lines show a simple pseudocode for the PSO algorithm based on the idealization presented above.

```

Initialize particles
For i=1 to max-iter
For each particle do
Evaluate fitness function
Find the  $P_{KBEST}$ ,  $G_{KBEST}$ 
end
end
for each particle do
update velocity & position
end
    
```

7. Particle swarm optimization algorithm

The controllers of conventional PI controller, PDMPI and PFOPI designed and compared with proposed PDMFOPI for the same system considered and simulated for 1% of SLP.

7.1 Design conventional PI controller

The output feedback ISE criterion is used in the design of traditional PI controllers for hybrid power systems. The obtained feedback gain values are $k_{p1} = 0.95$, $k_{i1} = 3.26$, $k_{p2} = 0.91$, $k_{i2} = 3.8$. The PI controller,

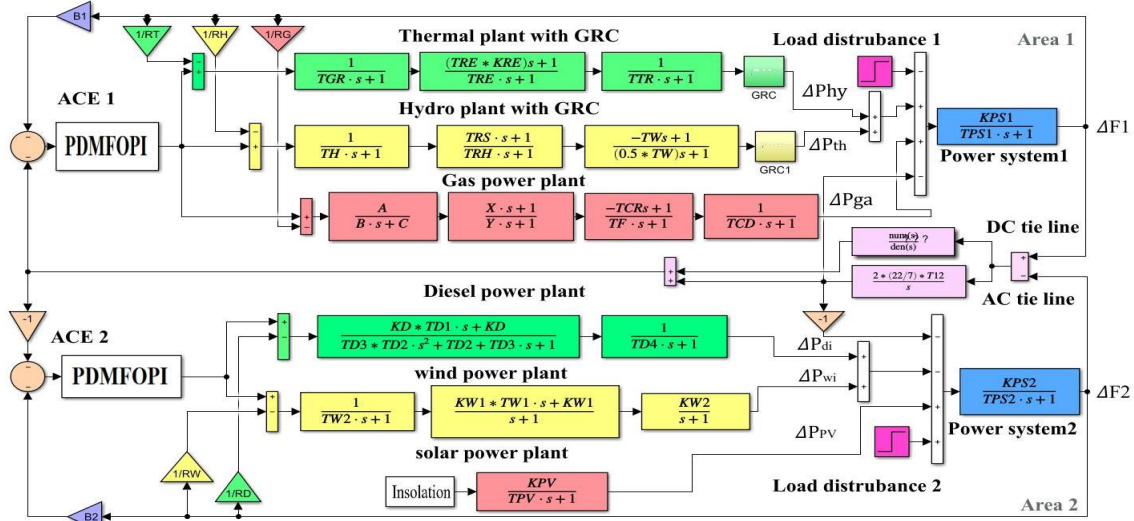


Figure. 4 Simulation model of TAIHS

PFOPi controller and PDMPI controller are used as a bench mark in this research work.

7.2 Design of proposed PDMFOPI controller

For TAIHS, the proposed PDMFOPI controller is constructed by incorporating the dual mode scheme and a fractional order controller. The parameters shown in Table I were initial parameters set for the good operation of the PSO algorithm. Also, upper and lower bounds for the controller gains to be tuned are also pre-set. According to the pseudo code of PSO algorithm, after initialization of particles, each particle starts to evaluate the fitness function, which is to find the controller gains in order to minimize the steady state error, thereby reducing the frequency deviation. Particles in the field look for the most suitable global and personal answers. And next each particle updates its position and velocity according to the solution. In that way, it will find the optimal gain values. The obtained optimal gain values, λ and ε were found to be $K_{p1} = 5.91$, $K_{i1} = 5.19$, $K_{p2} = 7.75$, $K_{i2} = 7.7$, $\lambda_1 = 0.71$, $\lambda_2 = 0.72$, $\varepsilon_1 = 0.35$, $\varepsilon_2 = 0.38$.

7.3 Design PFOPi and PDMPI controllers

A PFOPi and a PDMPI were also constructed in each area for TAIHS. For the PFOPi controller, the fractional order controller in each area is tuned with the PSO algorithm. Here, K_{p1} , K_{p2} , K_{i1} , K_{i2} , λ_1 , λ_2 are the 6 variables to be tuned. The best gain values and λ values are identified for PFOPi to be $K_{p1} = 0.33$, $K_{i1} = 1.20$, $K_{p2} = 0.2$, $K_{i2} = 1.58$, $\lambda_1 = 0.89$, $\lambda_2 = 0.58$. When it comes to the design of the PDMPI controller, it is very similar to the PDMFOPI controller design.

The procedural steps are the same as for a proposed controller. The main difference is that tuning of the PDMPI controller involves six variables,

which are: switching limits ε_1 , ε_2 , integral gains of K_{i1} , K_{i2} and proportional gains of K_{p1} , K_{p2} . While for the proposed PDMFOPI controller, there are a total of eight variables due to the presence of FO controller which are: switching limits ε_1 , ε_2 , integral gains of K_{i1} , K_{i2} and proportional gains of K_{p1} , K_{p2} and fractional operator λ_1 , λ_2 . In short, the proposed PDMFOPI controller has more control variables due to the presence of a fractional order controller and it produces a more precise output, therefore it has more control over the system to be controlled, while compared to the PDMPI controller, it has fewer variables. The obtained parameters for PDMPI are $\varepsilon_1 = 0.22$, $\varepsilon_2 = 0.27$, $K_{p1} = 0.9$, $K_{i1} = 1.2$, $K_{p2} = 0.84$, $K_{i2} = 9$, respectively.

8. Observations and simulation results

The TAIHS is simulated in the MatLab simulink platform as in Fig. 4 with the proposed PDMFOPI controller and other benchmark controllers for 1% SLP. The corresponding convergence curve and the associated output of frequency change of each area $\Delta F1$ and $\Delta F2$ as well as the tie line, which is displayed in Fig. 5 and Fig. 6. The Table 2 shows the numerical output data for the TAIHS with various controllers in terms of undershoot, overshoot and settling time and performance index produced by employing benchmark controllers and the proposed controller. The performance index obtained for the controllers also displayed in Table 3 which is also compared with the previous work by using algorithms of Differential Evolution (DE) algorithm, Artificial electric field (AEFA) and combinational of differential evolution-artificial electric field (DE-AEFA).

It is obvious from the results that the suggested PDMFOPI controller has a minimal ISE of 0.0084

Table 2. Numerical outcomes of controllers

	Controller Type	Undershoot	Overshoot	Settling time (Secs)* 10^{-2}
ΔF_1 in Hz	PI	-0.4385	1.2120	3.4468
	PDMPI	-0.4934	2.1260	2.4026
	PFOPi	-0.4507	0.7385	2.8903
	PDMFOPI	-0.4322	0.1812	0.7783
ΔF_2 in Hz	PI	-0.2934	1.242	3.2707
	PDMPI	-0.2491	2.132	2.3852
	PFOPi	-0.1538	0.7348	2.8185
	PDMFOPI	-0.08501	0.1589	2.2580
ΔT_{12} in MW	PI	-0.324	0.04297	2.2514
	PDMPI	-0.4869	0.1007	1.4962
	PFOPi	-0.3231	0.0248	1.0366
	PDMFOPI	-0.3879	0.0230	0.8744

Table 3. Performance index (ISE) of different controllers

Controller Type	ISE	Controller Type	ISE
PI	0.4386	AEFA [25]	23.478
PFOPi	0.11062	DE-AEFA [25]	12.416
PDMPI	0.6057	PDMFOPI	0.0084
DE [25]	25.725		

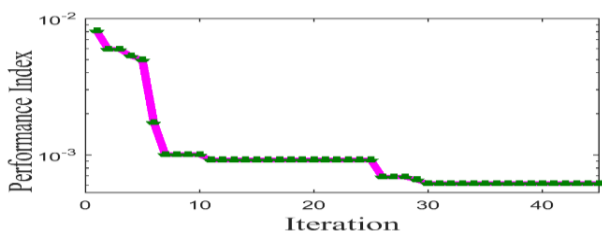
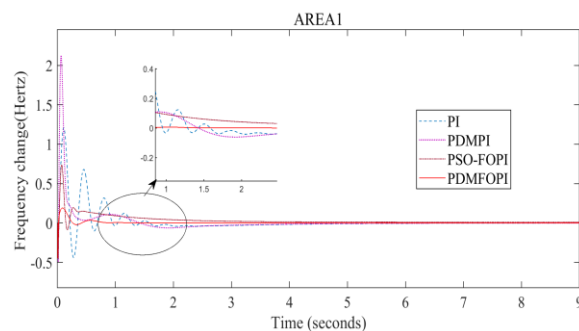


Figure. 5 Convergence curve

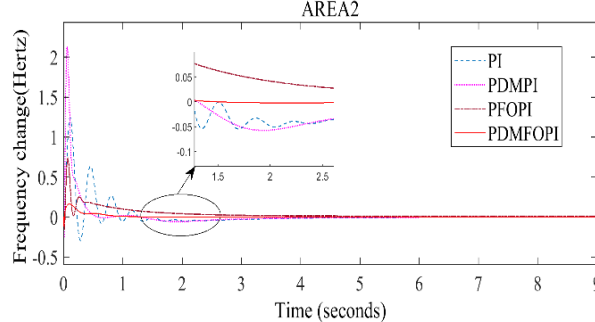
than the other compared controllers. The results from Table 2 shows that the suggested PDMFOPI controller has reduced undershoot, overshoot, less settling time and from the Table 3 it is clear that the minimal performance index is obtained on comparing the other controllers.

8.1 Sensitivity analysis with parameter variation

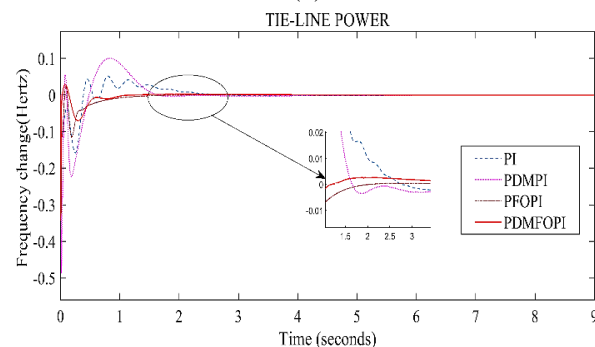
The characteristics of the hybrid system are altered to confirm the proposed controller's superiority and validity. A sensitivity analysis is performed on a two-area hybrid system by varying K_{PV} of the solar PV and the T_{CD} of the gas power plant in area 2 and 1 by $\pm 25\%$. The corresponding simulated results are given in Fig. 7 and 8. The suggested PDMFOPI controller appears to be impervious to parameter changes based on the simulation results.



(a)



(b)



(c)

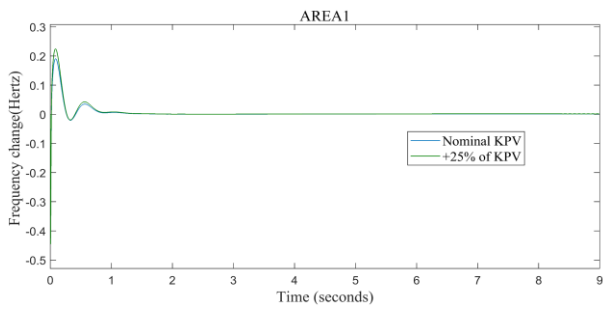
Figure. 6 Frequency change in: (a) area1, (b) area2, and (c) tieline

8.2 Performance analysis by considering AC links only

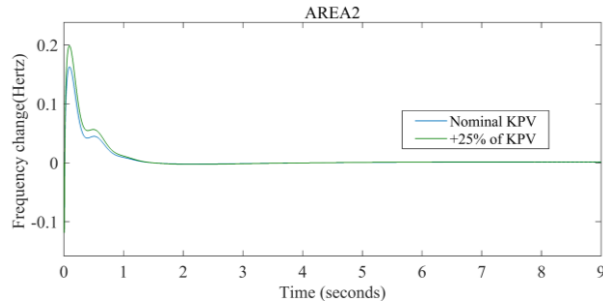
In the TAIHS, an HVDC link is built in parallel to the AC tie line to improve the frequency regulation, thereby improving the system performance. It is also important to discuss the system in the absence of the HVDC link due to technical faults. In that aspect, the TAIHS is simulated and the associated output is depicted in Fig. 9. From the result, it is clear that the system not get affected with the proposed controller with minimal variations.

8.3 Performance analysis with an electric governor

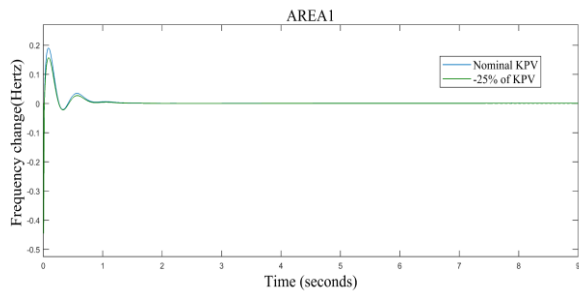
Mechanical regulators were once utilized in several of the existing thermal power plants. As a result of the faster growth of scientific study, electrical governors are now utilized to accomplish



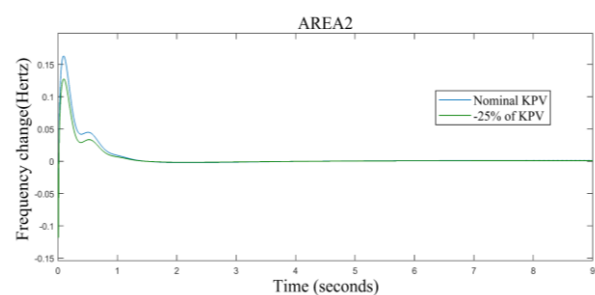
(a)



(b)

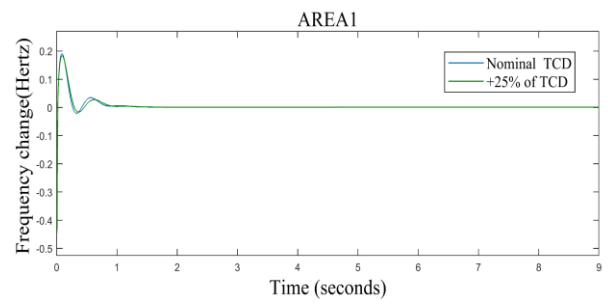


(c)

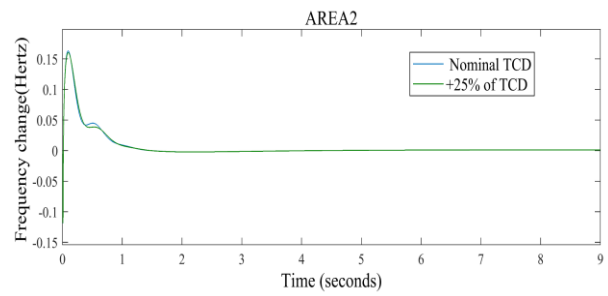


(d)

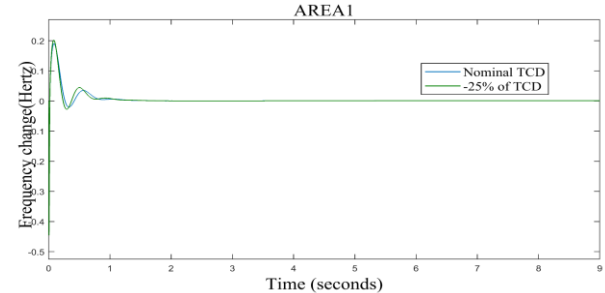
Figure. 7 Frequency change for +25% of KPV in: (a) area1, (b) area2, and -25% of KPV in (c) area1, and (d) area2



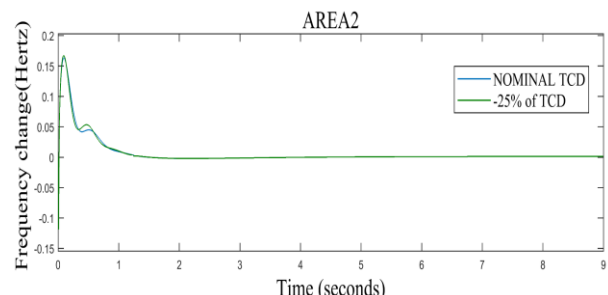
(a)



(b)

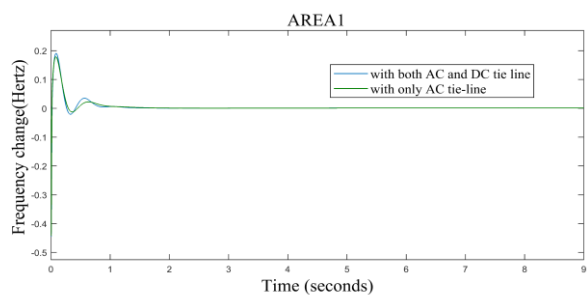


(c)

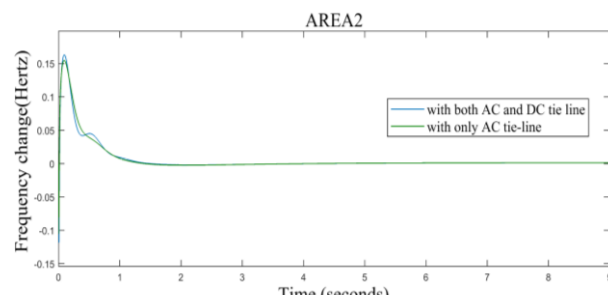


(d)

Figure. 8 Frequency change for +25% of Tcd in: (a) area1, (b) area2, and -25% of Tcd in (c) area1, and (d) area2



(a)



(b)

Figure. 9 Frequency change in: (a) area1 and (b) area2

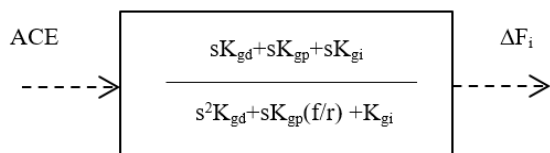


Figure. 10 Transfer function of electric governor

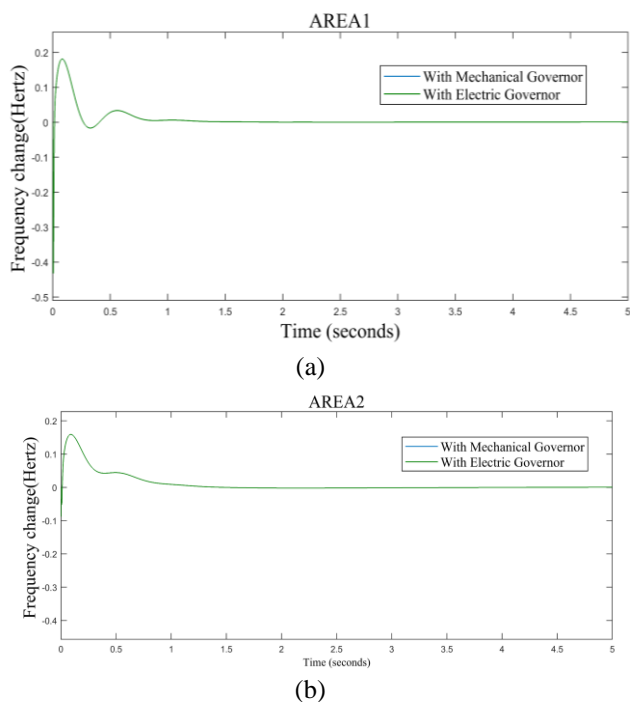


Figure. 11 Frequency change in: (a) area1 and (b) area2

activities such as speed detection and droop correction. If the mechanical governor is replaced with an electrical governor, it is necessary to investigate the system's performance. In this case, an electric governor is employed instead of a mechanical governor, Transfer function of electric governor is given in Fig. 10.

Were K_{gd} , K_{gi} , K_{gp} derivative, integral and proportional gains of the electric governor. And the corresponding output is displayed in Fig. 11. From these outputs, it is very clear that the system is well performed even with the replaced electric governor.

9. Conclusions

In this article, the PDMFOPI controller is described for the load frequency control of TAIHS. The proposed controller can handle complex system with good transient and steady-state performance because it combines two control schemes: the dual-mode and fractional order control. The performance analysis and sensitivity analysis also carried out for the TAIHS with the controller and compared with some other controllers. The conclusion points are as follows.

- In the TAIHS, the proposed PDMFOPI controller tuned by the PSO algorithm achieved the minimum ISE value of 0.0084 for 1% of SLP in both areas of the hybrid system.
- The proposed PDMFOPI controller achieved the least settling time, undershoot, and overshoot when compared with other controllers of the conventional PI controller, the PDMPI controller, and the PFOPI controller.
- From the sensitivity analysis, it is proven that the controller worked in an excellent way even with the parameter variation in the system.
- The system's performance is unaffected by the presence of an electric governor or the absence of an HVDC line due to a fault.

Finally, in terms of frequency change in each area and tie-line, the obtained waveforms and tabulation results confirmed the superiority and soundness of the PDMFOPI controller over the other compared benchmark controllers for the TAIHS.

Conflicts of Interest

The authors declare no conflict of interest.

Author Contributions

The draft has been prepared by the 1st author while the review and editing has performed by the 2nd author.

References

- [1] D. Sharma, "Load Frequency Control: A Literature Review", *International Journal of Scientific & Technology Research*, Vol. 9, pp.6421-6437, 2020.
- [2] B. P. Sahoo and S. Panda, "Load Frequency Control of Solar PV/Wind/Biogas/Biodiesel Generator Based Isolated Microgrid Using Harris Hawks Optimization", In: *Proc. of First International Conference on Power, Control and Computing Technologies*, pp. 188-193, 2020.
- [3] R. Mandal and K. Chatterjee, "Frequency control and sensitivity analysis of an isolated microgrid incorporating fuel cell and diverse distributed energy sources", *International Journal of Hydrogen Energy*, Vol. 45, No. 23, pp. 13009-13024, 2020.
- [4] B. Vedik, R. Kumar, R. Deshmukh, S. Verma, and C. K. Shiva, "Renewable Energy-Based Load Frequency Stabilization of Interconnected Power Systems Using Quasi-Oppositional Dragonfly Algorithm", *Journal of Control*,

- Automation and Electrical Systems*, Vol. 32, No. 1, pp. 227-243, 2021.
- [5] M. Tarkeshwar, H. Malik, V. Mukherjee, A. A. Majed and A. Almutairi, "Renewable generation based hybrid power system control using fractional order-fuzzy controller", *Energy Reports*, Vol. 7, pp. 641-653, 2021.
- [6] K. Amir, S. Soleymani, B. Mozafari, and M. Fotuhi, "Integrated multi-area power system with HVDC tie-line to enhance load frequency control and automatic generation control", *Electrical Engineering*, Vol. 102, No. 3, pp. 1223-1239, 2020.
- [7] T. Mehdi, E. Pouresmaeil, J. Adabi, R. Godina, and J. P. S. Catalão, "Load-frequency control in a multi-source power system connected to wind farms through multi terminal HVDC systems", *Computers and Operations Research*, Vol. 96, pp. 305-315, 2018.
- [8] D. Guha, P. K. Roy, and S. Banerjee, "Grasshopper optimization algorithm scaled fractional order PI-D controller applied to reduced order model of load frequency control system", *International Journal of Modelling and Simulation*, Vol. 40, No. 3, pp. 217-242, 2020.
- [9] A. Widi, S. Muslim, B. Suprianto, S. Haryudo, and A. C. Hermawan, "Intelligent Control of Power System Stabilizer Based on Archimedes Optimization Algorithm - Feed Forward Neural Network", *International Journal of Intelligent Engineering and Systems*, Vol. 14, No. 3, pp. 43-53, 2021, doi: 10.22266/ijies2021.0630.05.
- [10] M. W. Firdaus, S. M. Zoqi, R. Asyrofa, and W. A. Wahyu, "Optimization of Multi-Stage Distribution Process Using Improved Genetic Algorithm", *International Journal of Intelligent Engineering and Systems*, Vol. 14, No. 2, pp. 211-219, 2021, doi: 10.22266/ijies2021.0430.19.
- [11] S. Amin, F. Babaei, and F. Meisam, "A load frequency control using a PSO-based ANN for micro-grids in the presence of electric vehicles", *International Journal of Ambient Energy*, Vol. 42, No. 6, pp. 688-700, 2021.
- [12] Y. A. Dahab, H. Abubakr, and T. H. Mohamed, "Adaptive load frequency control of power systems using electro-search optimization supported by the balloon effect", *IEEE Access*, Vol. 8, pp. 7408-7422, 2020.
- [13] J. Guo, "Application of a novel adaptive sliding mode control method to the load frequency control", *European Journal of Control*, Vol. 57, pp. 172-178, 2021.
- [14] H. Mina, N. Reza, J. Saeid, and S. Hossein, "Optimal design of CDM controller to frequency control of a realistic power system equipped with storage devices using grasshopper optimization algorithm", *ISA Transactions*, Vol. 97, pp. 202-215, 2020.
- [15] G. Arabinda, A. K. Ray, N. Md, and J. Mo, "Voltage and frequency control in conventional and PV integrated power systems by a particle swarm optimized Ziegler-Nichols based PID controller", *SN Applied Sciences*, Vol. 3, No. 3, pp. 1-13, 2021.
- [16] C. A. Monje, B. M. Vinagre, V. Feliu, and Y. Q. Chen, "Tuning and auto-tuning of fractional order controllers for industry applications", *Control Engineering Practice*, Vol. 16, No. 7, pp. 798-812, 2008.
- [17] B. Kishore, I. Rosdiazli, K. M. Noh, H. S. Miya, and H. V. Rajah, "Fractional-order systems and PID controllers", *Springer International Publishing*, 2020.
- [18] E. A. Mohamed, E. M. Ahmed, A. Elmelegi, M. Aly, O. Elbaksawi, and A. A. A. Mohamed, "An Optimized Hybrid Fractional Order Controller for Frequency Regulation in Multi-Area Power Systems", *IEEE Access*, Vol. 8, pp. 213899-213915, 2020.
- [19] N. K. Jena, S. Sahoo, A. Naik, B. K. Sahu, and K. Mohanty, "Frequency Control of an AC Microgrid with Fractional Controller", *Green Technology for Smart City and Society*, pp. 277-288, 2021.
- [20] M. Ardashir and E. Kayacan, "A novel fractional-order type-2 fuzzy control method for online frequency regulation in ac microgrid", *Engineering Applications of Artificial Intelligence*, Vol. 90, pp. 103483, 2020.
- [21] K. Singh, "Load frequency regulation by de-loaded tidal turbine power plant units using fractional fuzzy based PID droop controller", *Applied Soft Computing Journal*, Vol. 92, 2020.
- [22] M. T. A. Mustafa and S. Velusami, "Dual mode linguistic hedge fuzzy logic controller for an isolated wind-diesel hybrid power system with superconducting magnetic energy storage unit", *Energy Conversion and Management*, Vol. 51, No. 1, pp. 169-181, 2010.
- [23] S. Velusami and I. A. Chidambaram, "Design of decentralized biased dual mode controllers for load-frequency control of interconnected power systems", *Electric Power Components and Systems*, Vol. 34, No. 10, pp. 1057-1075, 2006.
- [24] K. S. Simhadri and B. Mohanty, "Performance analysis of dual-mode PI controller using quasi-oppositional whale optimization algorithm for load frequency control", *International Transactions on Electrical Energy Systems*, Vol. 30, No. 1, pp. 2159, 2020.

- [25] C. H. N. S. Kalyan and G. S. Rao, "Frequency and Voltage stabilisation in combined load frequency control and automatic voltage regulation of multiarea system with hybrid generation utilities by AC/DC links", *International Journal of Sustainable Energy*, Vol. 39, No. 10, pp. 1009-1029, 2020.
- [26] S. P. Nangrani and S. S. Bhat, "Fractional Order Controller for Controlling Power System Dynamic Behaviour", *Asian Journal of Control*, Vol. 20, No. 1, pp. 403-414, 2018.
- [27] D. Sharma and N. K. Yadav, "LFOPI controller: a fractional order PI controller based load frequency control in two area multi-source interconnected power system", *Data Technologies and Applications*, Vol. 54, No. 3, pp. 323-342, 2020.
- [28] S. R. Manickam and M. T. A. Mustafa, "Design of biogeography optimization based dual mode gain scheduling of fractional order PI load frequency controllers for multi source interconnected power systems", *International Journal of Electrical Power and Energy Systems*, Vol. 83, pp. 364-381, 2016.

Appendix

In TAIHS [25], thermal plant: $T_{GR} = 0.08$ s; $T_{RE} = 10$ s; $K_{RE} = 0.3$; $T_{TR} = 0.3$ s; $R_T = 2.4$ For hydro plant: $T_H = 0.3$ s; $T_{RS} = 5$ s; $T_{RH} = 0.3$ s; $T_W = 0.025$ s; $R_H = 2.4$ For gas plant: $T_{CD} = 0.2$; $T_F = 0.23$ s; $T_{CR} = 0.01$; $R_G = 2.4$ A = 1; B = 0.05; C = 1; X = 0.6; Y = 1; diesel plant: $T_{D1} = 1$ s; $T_{D2} = 2$ s; RD = 2.4; $T_{D3} = 0.025$ s; $T_{D4} = 3$ s; $K_D = 16.5$. wind plant: $T_{W1} = 0.6$ s; $T_{W2} = 0.041$ s; $K_{W2} = 1.4$; $K_{W1} = 1.25$; $R_W = 2.4$ For solar PV plant: $K_{PV} = 1$; $T_{PV} = 1.8$.power system: Pr Rated power = 2000 MW, $T_{PS2} = 2 * (5/60 * 0.0145)$; $K_{PS1} = (1/0.0145)$; $K_{PS2} = (1/0.0145)$; $B_1 = 0.425$; $B_2 = 0.045$; $T_{12} = 0.545$ s; D = 0.0145, H = 5; f = 60 Hz; $K_{PS} = 1/D$; $T_{PS} = 2H/fD$; DC tie-line: $K_{DC} = 1$; $T_{DC} = 0.5$; AC tie-line: $T_{12} = 0.545$.Electric governor: $K_{pei} = 1.0$; $K_{iei} = 5.0$; $K_{dei} = 4.0$; R = 2.4 Hz/p.u.MW.

Notation

ACE_{A1}, ACE_{A2}	Area control error in area1 and area2
PSO	Particle swarm optimization
PDMPI	PSO based proportional integral controller
PFOPI	PSO based fractional order controller
PDMFOPI	PSO based dual mode fractional order controller
TAIHS	Three area interconnected hybrid system
ΔP_{tie12}	Change in tie-line power
$U(t)$	Control signal
$e(t)$	Error signal
$\Delta P_{tac}, \Delta P_{tdc}$	Change in Ac tie line power and DC tie line power
ΔP_{GEN1}	Power generated in area 1
ΔP_{GEN2}	Power generated in area 2
B1, B2	Biasing coefficient in area 1 area 2
λ	Fractional operator
ϵ	Switching limit
$\Delta F1, \Delta F2$	Frequency change in area1, area2
K_i, K_p	Integral gain and proportional gain
SLP	Step load perturbation
$\Delta P_{th}(s)$	Change in Thermal power for small change in SLP
$\Delta P_{hy}(s)$	Change in Hydropower for small change in SLP
$\Delta P_{ga}(s)$	Change in Gas power for small change in SLP
$\Delta P_{wi}(s)$	Change in Wind power for small change in SLP
$\Delta P_{pv}(s)$	Change in Solar power for small change in SLP
$\Delta P_{di}(s)$	Change in diesel power for small change in SLP